The FASEB Journal express article 10.1096/fj.03-1204fje. Published online March 19, 2004.

Impaired liver regeneration in mice lacking methionine adenosyltransferase 1A

Lixin Chen[*] Ying Zeng,[*] Heping Yang,[*] Taunia D. Lee,[*] Samuel W. French,[†] Fernando J. Corrales,[‡] Elena R. García-Trevijano,[‡] Matías A. Avila,[‡] José M. Mato,[§] and Shelly C. Lu[*]

[*]Division of Gastroenterology and Liver Diseases, USC-UCLA Research Center for Alcoholic Liver and Pancreatic Diseases, USC Research Center for Liver Diseases, USC School of Medicine, Los Angeles, California 90033; [†]Department of Pathology, Harbor-UCLA Research and Education Institute, 1000 West Carson Street, Torrance, California 90502; [‡]Fundación para la Investigación Médica Aplicada (FIMA), University of Navarra, Pamplona, Spain; [§]CIC-Biogune, Metabolomics Unit, Building 801a, Technological Park, 48160 Derio, Bizkaia, Spain

Corresponding author: Shelly C. Lu, Division of Gastrointestinal and Liver Diseases HMR Bldg., 415 Department of Medicine USC School of Medicine 2011 Zonal Ave., Los Angeles, CA, 90033. E-mail: shellylu@usc.edu

ABSTRACT

Methionine adenosyltransferase (MAT) is an essential enzyme because it catalyzes the formation of S-adenosylmethionine (SAMe), the principal biological methyl donor. Of the two genes that encode MAT, *MAT1A* is mainly expressed in adult liver and *MAT2A* is expressed in all extrahepatic tissues. Mice lacking *MAT1A* have reduced hepatic SAMe content and spontaneously develop hepatocellular carcinoma. The current study examined the influence of chronic hepatic SAMe deficiency on liver regeneration. Despite having higher baseline hepatic staining for proliferating cell nuclear antigen, *MAT1A* knockout mice had impaired liver regeneration after partial hepatectomy (PH) as determined by bromodeoxyuridine incorporation. This can be explained by an inability to up-regulate cyclin D1 after PH in the knockout mice. Upstream signaling pathways involved in cyclin D1 activation include nuclear factor κB (NFκB), the c-Jun-N-terminal kinase (JNK), extracellular signal-regulated kinases (ERKs), and signal transducer and activator of transcription-3 (STAT-3). At baseline, JNK and ERK are more activated in the knockouts whereas NFκB and STAT-3 are similar to wild-type mice. Following PH, early activation of these pathways occurred, but although they remained increased in wild-type mice, c-jun and ERK phosphorylation fell progressively in the knockouts. Hepatic SAMe levels fell progressively following PH in wild-type mice but remained unchanged in the knockouts. In culture, *MAT1A* knockout hepatocytes have higher baseline DNA synthesis but failed to respond to the mitogenic effect of hepatocyte growth factor. Taken together, our findings define a critical role for SAMe in ERK signaling and cyclin D1 regulation during regeneration and suggest chronic hepatic SAMe depletion results in loss of responsiveness to mitogenic signals.

Key words: S-adenosylmethionine • partial hepatectomy • cyclin D1 • hepatocyte growth factor

Methionine is an essential amino acid metabolized mainly by the liver, where it is converted, by the enzyme methionine adenosyltransferase (MAT), into S-adenosylmethionine (SAMe), the main biological methyl donor, precursor for polyamines and GSH (1). About 50% of methionine metabolism and up to 85% of all methylation reactions occur in the liver (2). In mammals, there are two genes encoding MAT isoenzymes: MAT I/III are gene products of *MAT1A*, and MAT II is the gene product of *MAT2A*. Whereas *MAT1A* is expressed mainly in the adult liver and is a marker for differentiated liver, *MAT2A* is expressed in all tissues, including fetal liver, hepatocellular carcinoma (HCC), and, in small quantities, in the adult liver (2). *MAT2A* is up-regulated during rapid liver growth and de-differentiation (2). Due to differences in the regulatory and kinetic properties of the various MATs, MAT II cannot maintain the same high levels of SAMe as compared with the combination of MAT I and MAT III (2). Consequently, in *MAT1A* knockout mice, despite a significant increase in *MAT2A* expression, the liver content of SAMe is reduced about threefold from birth, when the switch from *MAT2A* and *MAT1A* normally takes place (3).

It has long been realized that patients with cirrhosis often have hypermethioninemia and delayed plasma clearance of methionine after an i.v. injection (4). This is due to reduced hepatic MAT activity as a result of decreased *MAT1A* expression and inactivation of its gene products MAT I/III (5, 6). Thus, the biosynthesis of hepatic SAMe is impaired in cirrhotic patients, which can lead to reduced transmethylation and GSH synthesis (2). This may explain the finding that SAMe treatment of cirrhotic patients resulted in restoration of hepatic GSH levels (7). The *MAT1A* knockout mouse model exhibits abnormalities that mimic human cirrhotics, namely hypermethioninemia, chronic hepatic SAMe, and GSH deficiency (3), and serves as an excellent tool to examine the consequences of such deficiencies.

Using the *MAT1A* knockout mouse model, we have described two major consequences of chronic hepatic SAMe deficiency. The first is the predisposition of these animals to develop liver injury either in response to a choline-deficient diet or carbon tetrachloride, or spontaneous development of steatohepatitis (3, 8). The second is abnormal hepatic growth, resulting in spontaneous development of HCC (3, 8). SAMe deficiency is a well-known consequence of diets deficient in lipotropes and may be the underlying mechanism of steatohepatitis and HCC development in rodents fed such diets (9).

Accumulating evidence suggests SAMe is an important modulator of hepatocyte growth (2, 8, 13, 14). Whereas chronic hepatic SAMe deficiency leads to malignant degeneration (8), a transient fall in hepatic SAMe level precedes liver regeneration after 2/3 partial hepatectomy (PH) (10) and is necessary for normal regeneration to occur (11, 12). The mechanism may lie in the ability of SAMe to inhibit the mitogenic effect of hepatocyte growth factor (HGF), which was demonstrated using cultured rat hepatocytes (13). In this experimental model, the mitogenic effect of HGF requires inducible nitric oxide synthase (iNOS), which is also induced after PH (14). Because MAT I/III can be inhibited by nitrosylation (2), one plausible scenario is that increased iNOS expression that occurs soon after PH leads to increased nitric oxide levels and inhibition of MAT I/III. This in turn results in lower hepatic SAMe levels and release of the inhibitory effect that this molecule exerts on the proliferative activity of HGF. This mechanism would not work in the *MAT1A* knockout mouse because MAT II is not subject to nitrosylation and inactivation (2). How the liver responds to PH in this setting is unknown and forms the subject of the current work. This has direct relevance to human liver disease because a

significant proportion of cirrhotics have undetectable *MAT1A* expression, presumably due to hypermethylation of the *MAT1A* promoter (6).

MATERIALS AND METHODS

Partial hepatectomy experiments

Two-third hepatectomy experiments were performed using 2- to 3-month-old male wild-type mice and *MAT1A* knockout mice (3). Mice were fed ad libitum a standard diet (Harland Teklad irradiated mouse diet 7912, Madison, WI) and housed in a temperature-controlled animal facility with 12 h light-dark cycles. Animals were treated humanely, and all procedures were in compliance with our institutions' guidelines for the use of laboratory animals. Two-third PH was done according to the method of Higgins and Andersen (15) between 8 and 11 a.m. There was no operative mortality. Liver specimens removed represented time zero and were snap frozen in liquid nitrogen or formalin fixed for subsequent analysis as described below. Animals were allowed to recover for up to 72 h without postoperative mortality. Groups of animals (n=3–5 each) were killed at 0.5 h, 24 h, 36 h, 48 h, and 72 h. Two h before they were killed, mice were injected i.p. with bromodeoxyuridine (BrdU, 100 mg/kg body weight) to assess hepatocyte DNA synthesis. For the groups that were killed at 0.5 h, animals received BrdU injection 2 h before PH. The liver resected at the time of PH from this group formed the baseline BrdU values. At the time of sacrifice, livers were weighed and rapidly split into several pieces, some were snap frozen for subsequent RNA or protein extraction; others were formalin fixed for histology and immunohistochemistry as described below.

Liver histology and immunohistochemistry

Sections from formalin-fixed and paraffin-embedded liver tissue were stained with mouse monoclonal anti-BrdU antibody (Sigma, St. Louis, MO), 1:1000 dilution, at 4°C overnight. Secondary antibody was peroxidase-labeled goat anti-mouse antibody (Dako Envision System Carpinteria, CA) incubated at room temperature for 30 min. Hepatic nuclear BrdU incorporation was evaluated by two observers blinded to the animal's identity and treatment. BrdU incorporation was measured by the number of BrdU (+) nuclei in 10 microscope fields using a 40× objective and a 10× eyepiece with a Nikon 400 microscope and Morphometric software. Proliferating cell nuclear antigen (PCNA) expression was evaluated in a similar manner, using mouse monoclonal anti-PCNA primary antibody, followed by peroxidase-labeled goat anti-mouse antibody (Dako Envision System) at room temperature for 3 h, stained with peroxidase substrate (dab) 3,3′-diamino-benzidine chromagen (Dako) and counterstained with hematoxylin. PCNA expression was measured by the number of PCNA (+) nuclei in 10 microscope fields (×400) in each specimen. Finally, apoptosis was evaluated in these liver specimens using the TUNEL assay performed according to the manufacturer's instructions (In Situ Cell Death Detection Kit; Boehringer Mannheim, Indianapolis, IN) and using the same morphometric analysis as above.

Cell culture experiments

Hepatocyte isolation and DNA synthesis were measured as previously described (14). Hepatocytes were isolated from 3-month-old *MAT1A* knockout and wild-type mice as previously

described (14). Cultures were maintained in MEM medium supplemented with 5% fetal bovine serum (FBS), nonessential amino acids, 2 mmol/l glutamine, and antibiotics (Gibco-BRL, Carlsbad, CA). Medium was changed, and in the absence of serum, DNA synthesis was measured in response to varying concentrations of HGF (6.25, 12.5, and 25 ng/ml) for 36 and 72 h. A pulse of [^{3}H]thymidine (1μ Ci/well) was started 28 h after HGF addition. Cells were harvested, and thymidine incorporation was determined in a scintillation counter.

RNA isolation and gene expression analysis

Total liver RNA was isolated by the guanidinium thiocyanate method. RNA concentration was determined spectrophotometrically before use, and the integrity was checked by electrophoresis with subsequent ethidium bromide staining. Electrophoresis of RNA, gel blotting, and Northern hybridization analysis were performed on total RNA using standard procedures as previously described (3). Specific *MAT1A*, *MAT2A*, and 18S rRNA probes were labeled with [^{32}P]dCTP using a random primer kit (RediPrime DNA Labeling System; Amersham Pharmacia Biotech Piscataway, NJ) as previously described (3). Autoradiography and densitometry (Gel Documentation System, Scientific Technologies, Carlsbad, CA, and NIH Image 1.60 software program) were used to quantitate relative RNA. Results of Northern blot analysis were normalized to 18S rRNA.

For genes with low levels of expression, reverse-transcription polymerase chain reaction (RT-PCR) was used to assess their expression. These genes include iNOS, uncoupling protein 2 (UCP2), tumor necrosis factor α (TNF-α), and interleukin 6 (IL-6). One microgram of total RNA was subjected to reverse transcription using Superscript II reverse transcriptase (Invitrogen, Carlsbad, CA) and oligo(dT) as the priming agent. After 1 h incubation at 43°C, the reactions were stopped by heating at 70°C for 15 min. Template RNA was then removed using RNase H (Invitrogen). Ten percent of the reverse transcriptase reaction was amplified using primers for iNOS (5′-CAGGGAATCTTGGAGCGAGTTGTGG-3′ sense and 5′-CCCGTACCAGGCCCAATGAG GAT-3′ antisense, which corresponds to nucleotides 2406 to 3007 of the iNOS gene [16]), UCP2 (5′-ACTTCTCCCAATGTTGCCCG-3′ sense and 5′-GACTGGGCAGAGGATGAAG -3′ antisense, which corresponds to nucleotides 897 to 1344 of the UCP2 gene [17]), TNF-α (18), and IL-6 (19). 18S rRNA was amplified simultaneously using QuantumRNA Classic II 18 s (Ambion, Austin, TX) for internal control of RNA loading. The PCR condition for iNOS was 38 cycles (94°C, 45 s; 68°C, 45 s; 72°C, 45 s), for UCP2 was 38 cycles (94°C, 45 s; 60°C, 45 s; 72°C, 45 s), for TNF-α was 38 cycles (94°C, 45 s; 60°C, 45 s; 72°C, 1min), and for IL-6 was 41 cycles (94°C, 45 s; 55°C, 1 min; 72°C, 1 min). Expression of these genes was normalized to 18S expression.

Western blot analysis

Liver homogenates were subjected to Western blot analysis as we previously described (3, 8, 14). Equal amounts of protein (50 μg/well) were resolved in 12.5% SDS-polyacrylamide gels. Proteins were electrophoretically transferred to nitrocellulose membranes, blocked with tris-buffered saline (pH 7.6)/0.1% Tween 20 containing 5% nonfat dried milk, washed with tris-buffered saline/0.1% Tween 20, and incubated 1.5 h with primary antibodies in tris-buffered saline/0.1% Tween 20 containing 5% nonfat dried milk. Blots were washed in tris-buffered saline/0.1% Tween 20 and incubated 45 min with the secondary antibody in tris-buffered saline/0.1% Tween 20 containing 5% nonfat dried milk. Membranes were probed with anti-MAT

I/III, anti-cyclin D1 (Santa Cruz Biotechnology, Santa Cruz, CA) 1:100, anti-phospho-extracellular signal-regulated kinase (ERK) (Cell Signaling Technology, Lexington, KY) 1:100, anti-ERK-2 1:500, anti-phospho signal transducer and activator or transcription-3 (STAT-3) 1:100, anti-STAT-3 1:500, anti-phospho-c-jun 1:500, anti-c-jun 1:500, anti-p65 or p50 1:200 antibodies (Santa Cruz Biotechnology). To ensure equal loading, we stained protein gels with Coomassie blue and/or stripped membranes and reprobed them with anti-actin antibodies (Santa Cruz Biotechnology). A horseradish peroxidase-conjugated secondary antibody was used. Blots were developed by enhanced chemoluminescence.

Electrophoretic mobility shift assay (EMSA) and supershift assay

Nuclear proteins were extracted from wild-type and knockout livers at time 0 and 24 h and subjected to EMSA for NFκB as previously described (20) using a consensus NFκB probe (Santa Cruz Biotechnology). Supershift analysis was done using anti-p50 antibodies as we previously described (20).

Hepatic ATP levels

Hepatic ATP levels were measured by luciferase assay using reagents from Sigma according to the manufacturer's instructions. Before the assay was performed, snap frozen liver specimens (50 mg/mouse) were pulverized in a mortar and pestle under liquid nitrogen, suspended in ice-cold lysis buffer, and centrifuged at 4°C for 5 min, and the supernatant was removed for measurement of luciferase activity using a TD-20/20 Luminometer (Promega, Madison, WI) at 37°C. ATP levels in the samples were determined by comparison with a concurrent standard curve and expressed as μg ATP/g liver.

Hepatic SAMe levels

Hepatic SAMe levels were measured using a method described previously (10) with slight modifications. Liver specimens were homogenized in phosphate-buffered saline, and an aliquot was saved for protein assay. The rest was treated with 100 μl of 1 M perchloric acid (PCA) on ice for 5 min and centrifuged at 1000*g* for 15 min at 4°. The aqueous layer was quantitatively removed, neutralized with 3 M KOH, and centrifuged at 3000*g* for 10 min at 4°C. SAMe levels were determined in the neutralized PCA extracts by HPLC (LC-10ATVP pump, SCL-10AVP system control, Shimadzu, Columbia MD) with a SPD-10AVP UV detector and a SIL-10ADVP autosampler (Shimadzu) using a Partisil SCX 10 μm column (25×0.44 cm i.d.; Whatman Chem. Sep. Maidstone, Cleveland, OH). SAMe was eluted isocratically at 1 ml/min with 0.19 M $NH_4H_2PO_4$ adjusted to pH 2.6 with 2 M H_3PO_4. SAMe levels were calculated using standard curve of SAMe prepared at the same time as the samples and are reported as nmol/mg protein.

Statistics

Two-tailed non-paired Student's *t* test was used for comparisons between two groups, ANOVA followed by Fisher's test was used for comparison of more than two groups. Significance was defined by $P < 0.05$.

RESULTS

Liver regeneration in the MAT1A knockout mice

Liver regeneration was assessed in the knockout and wild-type mice by using PCNA staining and BrDU incorporation. PCNA is an auxillary protein of DNA polymerase delta. Its expression is cell cycle dependent, being first detected in late G_1 and remains increased throughout the S phase and into the early postreplicative G_2 period (21). BrDU is a thymidine analog that is incorporated into DNA during DNA synthesis (21). Thus, whereas both are markers of cellular replication, only BrDU is a specific marker for the S phase. Figure 1*A* shows that peak BrDU incorporation occurred at 48 h after PH in the wild-type and knockout mice. However, the number of BrDU-positive hepatocytes was much lower in the knockout mice at both 48 and 72 h. Interestingly, although baseline hepatic PCNA staining was much higher in the knockout mice, it fell significantly after PH instead of increasing steadily as in the wild-type mice (Fig. 1*B*). Figure 2 depicts these changes immunohistologically. The impairment in liver regeneration is not due to liver cell death as necrosis was not seen histologically and apoptosis was not detected on TUNEL assay (data not shown).

MAT expression during liver regeneration

We had previously shown that *MAT1A* expression falls transiently just before peak DNA synthesis whereas *MAT2A* is induced during liver regeneration in the rat (10). Others have shown that *MAT2A* up-regulation is required for proliferation to occur (22). Northern and Western blot analyses show that *MAT1A* expression remains elevated up to 72 h after PH in mice (Fig. 3). Hepatic *MAT2A* expression is induced at baseline in the knockout mice as we showed previously (3) and remains elevated up to 72 h after PH in both knockout and wild-type mice. (Fig. 3).

Mechanism of impaired liver regeneration

Immediately following PH, adult hepatocytes enter into a state of prereplicative competence before they can fully respond to growth factors. This priming step is thought to be mediated partly by an early release of TNF-α and IL-6, resulting in the activation of NFκB, c-Jun-N-terminal kinase (JNK), and STAT-3 and entry in G_1 phase (23, 24). These initiated cells are then able to further progress in early G_1 phase but require growth factor stimulation to progress beyond the restriction point in mid to late G_1 and enter S phase (23, 24). Although NFκB, JNK, and STAT-3 activation occur in early G_1, cyclin D1 is a delayed-early gene that is induced at the G_1-S boundary and required for progression from G_1 to S phase (24, 25). We next examined whether the activation of these pathways may be impaired in the *MAT1A* knockout mice following PH.

Figure 4 shows that TNF-α (Fig. 4*A*) and IL-6 (Fig. 4*B*) are induced in a similar manner in the knockouts as compared with wild-type mice. JNK activation as measured by level of phosphorylated c-jun is evident shortly after (30 min) PH in both wild-type and knockout mice (Fig. 5*A*). Note that the baseline level of phospho-c-jun is elevated in the knockout mice and although the level remains elevated in the wild-type mice, it fell progressively after this early increase in the knockout mice. By 36 h after PH, the level of phospho-c-jun was lower in the knockout as compared with wild-type mice (Fig. 5*A*). Changes in phospho-c-jun levels paralleled

changes in total c-jun levels (Fig. 5*A*). Similarly, NFκB activation as measured by the levels of p50 and p65 is also higher at baseline for the knockouts and increased shortly after PH (Fig. 5*B* and *C*). The level of p50 was not appreciably increased in the wild-type mice but was clearly induced in the knockouts at all time points examined after PH (Fig. 5*B*). The level of p65 increased progressively following PH in the wild-type mice but peaked at 30 min after PH in the knockouts (Fig. 5*C*). However, NFκB nuclear binding activity appeared comparable between wild-type and knockout mice at baseline and both were induced at 24 h after PH (Fig. 5*D*). Consistent with intact NFκB signaling is the observation that iNOS, a NFκB target gene (16), is similarly induced in both knockouts and wild-type mice (Fig. 4*C*). STAT-3 is a known downstream target of IL-6 that is also critical for normal liver regeneration to occur (26). This pathway appears to be intact in the *MAT1A* knockout mice (Fig. 6*A*).

JNK belongs to the family of stress-activated kinases and is one of multiple cellular signaling pathways activated shortly after PH (23, 27, 28). The other major signaling pathway activated is the mitogen-activated kinase (MAPK) pathway (23, 27, 28). ERKs are activated by phosphorylation, and two highly related MAPKs, p44 and p42, also called ERK1 and ERK2, are activated shortly after PH (24, 27, 17). Two peaks of ERK phosphorylation were observed after PH: one in early G_1, within 1 h of PH, and one in mid-late G_1, just preceding cyclin D1 mRNA induction (24). Figure 6*B* shows that ERKs are hyperphosphorylated at baseline in the knockout mice, and similar to the pattern observed with phospho-c-jun, the levels of phosphorylation decreased progressively in the knockout mice instead of increasing progressively as observed in the wild-type mice. At 36 h after PH before peak DNA synthesis, ERK phosphorylation was lower in the knockout as compared with wild-type mice (Fig. 6*B*). Total ERK2 levels were not different between knockout and wild-type mice and remained unchanged from baseline after PH (Fig. 6*B*).

Cyclin D1 induction is required for the G_1/S transition (23, 25, 28, 29). Upstream signaling pathways involved in cyclin D1 activation include NFκB, JNK, ERKs, and STAT-3 (29). Figure 6*C* shows that although cyclin D1 expression is doubled at baseline in the knockout mice, it failed to increase significantly after PH as compared with the wild-type mice. Cyclin D1 protein levels in the knockout livers were 6%, 15%, and 33% of wild-type livers at 24, 36, and 48 h after PH, respectively (Fig. 6*C*). Early activation of JNK, STAT3, and NFκB, coupled with the inability of the *MAT1A* knockout hepatocytes to up-regulate cyclin D1, suggests these hepatocytes are arrested in the prereplicative (G_1) phase of the cell cycle following PH.

Another factor important for cyclin D1/cyclin-dependent kinase activity is cellular ATP levels because ATP binding is required to activate the complex (27). This is an important consideration because we have shown that *MAT1A* knockout mice exhibit impaired hepatic mitochondrial function and have elevated UCP2 expression (8, 30). We confirmed that UCP2 expression is more than doubled at baseline in the knockout mice (Fig. 4*D*). However, UCP2 mRNA levels remained constant during liver regeneration in the knockout mice in contrast to the induction that occurred in the wild-type mice (Fig. 4*D*). Baseline hepatic ATP levels tended to be lower in the knockout mice and failed to increase at 36 h after PH as observed in the wild-type mice (Fig. 7).

To examine whether the impairment in regeneration may be due to loss of responsiveness to mitogenic signals, we isolated hepatocytes from wild-type and *MAT1A* knockout mice and measured DNA synthesis in response to varying concentrations of HGF. At baseline, knockout

hepatocytes had a 12.7-fold higher incorporation of thymidine than wild-type hepatocytes (wild type=1971±303, knockout=25,006±1281, expressed as mean±SD in unit of cpms/3×10^4 cells, $P<0.01$), which agrees with these cells being in a state of enhanced proliferation in the intact organ. Upon HGF treatment, wild-type hepatocytes showed a dose-dependent increase in thymidine incorporation into DNA (up to ~4.5-fold), whereas knockout hepatocytes had a minimal response (~1.5-fold) and showed no dose-dependency (Fig. 8). The response in the knockout hepatocytes was not merely delayed, because the same impaired effect of HGF on DNA synthesis was observed after 72 h of treatment (data not shown).

We had previously shown that SAMe inhibits the mitogenic effect of HGF on hepatocytes by an iNOS-dependent mechanism (14). This, coupled with the observation that hepatic SAMe levels fall after PH but before peak DNA synthesis (10), led us to speculate that the fall in SAMe may be due to NO-mediated inactivation of MAT I/III, which then releases the inhibitory tone of SAMe on HGF (14). This mechanism would not work in *MAT1A* knockout mice because MAT II is not subject to inactivation by NO (2). To examine this, we measured hepatic SAMe levels at various times after PH. In the wild-type animals, SAMe levels fell progressively from 24 to 48 h whereas they remained essentially unchanged in the knockout mice (Table 1).

DISCUSSION

Adult hepatocytes are normally quiescent (in G_0 phase) but retain enormous proliferative capacity when a deficit in hepatic mass occurs, such as following PH (23). Much has been learned about the mechanisms by which liver regeneration occurs, but there remains large gaps in many fundamental areas. One area addressed here is the effect of chronic hepatic SAMe deficiency on liver regeneration. This is a clinically relevant problem because cirrhotic patients have impaired hepatic SAMe biosynthesis due to decreased *MAT1A* expression and inactivation of MAT I/III (2, 6). Many cirrhotic patients have undetectable *MAT1A* expression, presumably due to promoter hypermethylation (6). The *MAT1A* knockout mouse model exhibits chronic hepatic SAMe deficiency (3) and represents an ideal model to address this question.

We have previously shown that in rodents, an early event after PH that precedes DNA synthesis is a transient fall in hepatic SAMe level (10). This could be partly attributed to an induction in the expression of *MAT2A*, which along with the fall in SAMe, has been shown by others to be necessary for hepatocyte proliferation to occur (10–12, 22). A potential mechanism for this is the ability of SAMe to modulate the activity of HGF. We have shown that SAMe inhibits the mitogenic effect of HGF, an effect that required iNOS (14). We hypothesized that following PH, the increase in nitric oxide production leads to inhibition of MAT I/III, leading to a fall in hepatic SAMe and release of the inhibitory tone this molecule exerts on the mitogenic activity of HGF (2, 14). However, this mechanism would not work in the *MAT1A* knockout mouse because MAT II is not subject to inactivation by nitric oxide (2). However, *MAT1A* knockout mice exhibit enhanced hepatic growth and develop spontaneous HCC (3, 8). How they respond to PH is of interest and the subject of current work.

MAT1A knockout mice exhibited an impaired regenerative response following PH. This is documented by a nearly 2/3 reduction in the number of BrDU positive hepatocytes at the time of peak DNA synthesis. There are two critical steps in liver regeneration: the transition of the quiescent hepatocyte into the cell cycle (priming) and the progression beyond the restriction

point in the G_1 phase of the cell cycle (23). Priming is believed to be largely attributed to TNF-α and IL-6, which then activate several signal transduction pathways, including NFκB, JNK, and STAT-3 in early G_1 phase (23, 24). Each of these pathways has been shown to be essential for liver regeneration to occur (23, 26, 28). Whereas priming is largely under the control of cytokines, progression in the G_1 phase and beyond the restriction point is believed to be controlled by growth factors such as HGF and transforming growth factor α (TGF-α) as well as cyclin D1 (23). Our data indicate that the early priming events appear to be intact in the knockout mice. Both TNF-α and IL-6 response are similar in the knockouts as compared with wild-type mice. This is consistent with early induction of NFκB, c-jun, and STAT-3. *MAT2A* and *iNOS*, two genes that have been shown to be essential for liver regeneration (22, 23), are also similarly induced in both types of mice. Intact iNOS response also suggests that NFκB signaling is not impaired in the knockout mice.

Our data indicate that there is a defect in the progression in G_1 phase in the *MAT1A* knockout hepatocytes and possibly a defect in response to growth factors. A critical factor in G_1 progression and up-regulation of cyclin D1 in mid-late G_1 phase is activation of ERK1/2 (24). We found ERK1/2 to be hyperphosphorylated and cyclin D1 expression higher in the knockout mice at baseline, consistent with an enhanced growth phenotype of these cells, as we previously reported (3, 8). However, following PH, ERK1/2 phosphorylation fell in the knockout mice and cyclin D1 failed to increase. This is consistent with arrest of the *MAT1A* knockout hepatocytes in the G_1 phase of the cell cycle. Interestingly, although acute MAPK cascade activation promotes G_1 progression and S phase entry, chronic activation of the MAPK cascade actually inhibits this process (32). Our data are consistent with this observation. JNK is also required for cyclin D1 expression (28). In the knockout mice, baseline JNK activity is enhanced, and although it increased shortly after PH, the increase was short-lived and, by 36 h after PH, it was lower than in wild-type mice. The reason for the inability to sustain JNK activation in the knockout mice is not clear, and it is also unclear whether this would have an impact on the course of regeneration. Another factor important for G_1 progression is ATP store (27). Hepatic ATP levels did not increase in the *MAT1A* knockout mice following PH, which is likely due to known impairment in hepatic mitochondrial function of these animals (30). It is possible that this also contributed to the impairment in G_1 progression. The mechanism of the blunted ATP response in the knockout mice is likely to be multifactorial. Both UCP-dependent and independent mechanisms are likely to be involved.

To investigate whether *MAT1A* hepatocytes have abnormal responsiveness to mitogenic signals, we used the cultured hepatocyte model to directly test the mitogenic effect of HGF. *MAT1A* hepatocytes have higher baseline DNA synthesis, which is consistent with a heightened proliferative state observed in vivo. However, little to no increase in DNA synthesis occurred in response to increasing doses of HGF, supporting the notion that one key abnormality in these hepatocytes is a loss in responsiveness to mitogens.

To test our hypothesis that loss of responsiveness to HGF may be due to the inability of NO to down-regulate MAT II in the *MAT1A* knockout mouse livers, we next measured hepatic SAMe levels. Consistent with this hypothesis, although hepatic SAMe levels fell progressively from 24 to 48 h in the wild-type animals, they remained essentially unchanged in the knockout livers.

Our findings are reminiscent of the impaired liver regeneration reported in ob/ob mice (27). Both *MAT1A* knockout mice and ob/ob mice have impaired cyclin D1 response following PH, and the hepatocytes are arrested in G_1. However, in the ob/ob mice, JNK and NFκB activation are impaired while ERK1/2 are superinduced (27). Thus, different mechanisms are responsible for the impaired cyclin D1 response. There are also similarities in our findings to those of the c-*myc* and TGF-α double transgenic mice (33). The double transgenic mice exhibit severe liver cell dysplasia and develop spontaneous liver neoplasms (33). Interestingly, the capacity of the transgenic livers to regenerate was markedly impaired following postnatal liver growth, which suggests early replicative senescence (33). The authors hypothesized that in these double transgenic mice, two alternative outcomes can occur with regard to growth potential: either an early loss of proliferative activity and eventual death or escape from a senescent pathway and rapid progression to an immortal tumor phenotype (33). A universal characteristic of senescent cells is the inability to respond to mitogenic signals (33). Given that the *MAT1A* knockout mice are predisposed to HCC and are unable to respond to mitogenic signals, the possibility of replicative senescence is real and deserves further study.

In summary, *MAT1A* knockout mice exhibit impairment in liver regeneration following PH. While the initial priming event appears to be intact, there is a defect in the progression in G_1 phase. This is due largely to the inability of cyclin D1 up-regulation, which may be related to the chronic activation of ERK1/2 and loss of response to growth factors possibly related to lack of a significant fall in hepatic SAMe levels. These findings have direct relevance to human liver cirrhosis where *MAT1A* is often silenced and hepatic SAMe store is depleted.

ACKNOWLEDGMENTS

This work was supported by grants from the National Institutes of Health: DK51719 (to S. C. Lu), AT1576 (to S. C. Lu, J. M. Mato, F. J. Corrales, and M. A. Avila), and AA13847 (to S. C. Lu, F. J. Corrales, and J. M. Mato); Plan Nacional de I+D 2002-00168 from Ministerio de Ciencia y Tecnología (to J. M. Mato); grants FIS 01/0712 and PI020369 from Ministerio de Sanidad y Consumo (to M. A. Avila and E. R. García-Trevijano, respectively); and 681/2000 from Gobierno de Navarra (to M. A. Avila). Grant FIT-090000-2003-109 from Ministerio de Ciencia y Tecnología (to F. J. Corrales, J. M. Mato, and M.A. Avila). Grants G03/015 and C03/02 from Instituto de Salud Carlos III (to J. M. Mato, M. A. Avila, and F. J. Corrales). This work has been funded in part by the FIMA and UTE/CIMA Project. T. D. Lee is a recipient of the Postdoctoral Fellowship of the Training Program in Alcoholic Liver and Pancreatic Diseases (T32 AA07578). The study was supported by Morphology Core of the Research Center for Alcoholic Liver and Pancreatic Diseases (P50 AA11999) funded by the National Institute on Alcohol Abuse and Alcoholism. We gratefully acknowledge Dr. Li Nan and Magdalena C. DeLeon for their technical support on immunohistologic staining and morphometric measurements, respectively.

REFERENCES

1. Cantoni, G. L. (1975) Biochemical methylations: selected aspects. *Annu. Rev. Biochem.* **44,** 435–441

2. Mato, J. M., Corrales, F. J., Lu, S. C., and Avila, M. A. (2002) S-Adenosylmethionine: a control switch that regulates liver function. *FASEB J.* **16,** 15–26

3. Lu, S. C., Alvarez, L., Huang, Z. Z., Chen, L., An, W., Corrales, F. J., Avila, M. A., Kanel, G., and Mato, J. M. (2001) Methionine adenosyltransferase 1 A knockout mice are predisposed to liver injury and exhibit increased expression of genes involved in proliferation. *Proc. Natl. Acad. Sci. USA* **98,** 5560–5565

4. Kinsell, L. W., Harper, H. A., Marton, H. C., Michael, G. D., and Weiss, H. A. (1947) Rate of disappearance from plasma of intravenously administered methionine in patients with liver damage. *Science* **106,** 589–590

5. Martin-Duce, A., Ortiz, P., Cabrero, C., and Mato, J. M. (1988) S-Adenosylmethionine synthetase and phospholipid methyltransferase are inhibited in human cirrhosis. *Hepatology* **8,** 65–68

6. Avila, M. A., Berasain, C., Torres, L., Martin-Duce, A., Corrales, F. J., Yang, H., Prieto, J., Lu, S. C., Caballeria, J., Rodes, J., et al. (2000) Reduced mRNA abundance of the main enzymes involved in methionine metabolism in human liver cirrhosis and hepatocellular carcinoma. *J. Hepatol.* **33,** 907–914

7. Vendemiale, G., Altomare, E., Trizio, T., Le Grazie, C., Di Padova, C., Salerno, M. T., Carrieri, V., and Albano, O. (1989) Effects of oral S-adenosyl-L-methionine on hepatic glutathione in patients with liver disease. *Scand. J. Gastroenterol.* **24,** 407–415

8. Martínez-Chantar, M. L., Corrales, F. J., Martínez-Cruz, A., García-Trevijano, E. R., Huang, Z. Z., Chen, L. X., Kanel, G., Avila, M. A., Mato, J. M., and Lu, S. C. (2002) Spontaneous oxidative stress and liver tumors in mice lacking methionine adenosyltransferase 1A. *FASEB J.* 10.1096/fj.02-0078fje

9. Newberne, P. M. (1986) Lipotropic factors and oncogenesis. *Adv. Exp. Med. Biol.* **206,** 223–251

10. Huang, Z. Z., Mao, Z., Cai, J., and Lu, S. C. (1998) Changes in methionine adenosyltransferase during liver regeneration in the rat. *Am. J. Physiol.* **38,** G14–G21

11. Pascale, R. M., Simile, M. M., Satta, G., Seddaiu, M. A., Daino, L., Pinna, G., Vinci, M. A., Gaspa, L., and Feo, F. (1991) Comparative effects of L-methionine, S-adenosyl-L-methionine and 5′-methylthioadenosine on the growth of preneoplastic lesions and DNA methylation in rat liver during the early stages of hepatocarcinogenesis. *Anticancer Res.* **11,** 1617–1624

12. Shivapurkar, N., Hoover, K. L., and Poirier, L. A. (1986) Effect of methionine and choline on liver tumor promotion by phenobarbital and DDT in diethylnitrosamine-initiated rats. *Carcinogenesis* **8,** 615–617

13. Latasa, M. U., Boukaba, A., GarcÌa-Trevijano, E. R., Torres, L., Rodríguez, J. L., Caballería, J., Lu, S. C., Lüpez-Rodas, G., Franco, L., Mato, J. M., and Avila, M. A. (2001)

Hepatocyte growth factor induces MAT2A expression and histone acetylation in rat hepatocytes. Role in liver regeneration. *FASEB J.* 10.1096/fj.00-0556fje

14. Garcia-Trevijano, E. R., Martínez-Chantar, M. L., Latasa, M. U., Mato, J. M., and Avila, M. A. (2002) NO sensitizes rat hepatocytes to hepatocyte growth factor-induced proliferation through the modulation of S-adenosylmethionine levels. *Gastroenterology* **122,** 1355–1363

15. Higgins, G. M., and Andersen, R. M. (1931) Experimental pathology of liver: restoration of liver of the white rat following partial surgical removal. *Arch. Pathol.* **12,** 186–202

16. Kone, B. C., Schwobel, J., Turner, P., Mohaupt, M. G., and Cangro, C. B. (1995) Role of NF-kappa B in the regulation of inducible nitric oxide synthase in an MTAL cell line. *Am. J. Physiol.* **269,** F718–F729

17. Horvath, B., Spies, C., Warden, C. H., Diano, S., and Horvath, T. L. (2002) Uncoupling protein 2 in primary pain and temperature afferents of the spinal cord. *Brain Res.* **955,** 260–263

18. Nomura, J., Hosoi, T., Okuma, Y., and Nomura, Y. (2003) Aβ-induced TNF-α expression and acetylcholine action in mouse glial cells. *Life Sci.* **72,** 2117–2120

19. Huang, Y. F., Harrison, J. R., Lorenzo, J. A., and Kream, B. E. (1998) Parathyroid hormone induces interleukin-6 heterogeneous nuclear and messenger RNA expression in murine calvarial organ cultures. *Bone* **23,** 327–332

20. Yang, H. P., Sadda, M. R., Yu, V., Zeng, Y., Lee, T. D., Ou, X. P., Chen, L. X., and Lu, S. C. (2003) Induction of human methionine adenosyltransferase 2A expression by tumor necrosis factor alpha: Role of NF-κB and AP-1. *J. Biol. Chem.* **278,** 50887–50896

21. Assy, N., and Minuk, G. Y. (1997) Liver regeneration: methods for monitoring and their applications *J. Hepatol.* **26,** 945–952

22. Pañeda, C., Gorospe, I., Herrera, B., Nakamura, T., Fabregat, I., and Varela-Nieto, I. (2002) Liver cell proliferation requires methionine adenosyltransferase 2A mRNA up-regulation. *Hepatology* **35,** 1381–1391

23. Fausto, N. (2000) Liver Regeneration. *J. Hepatol.* **32, Suppl. 1,** 19–31

24. Talarmin, H., Rescan, C., Cariou, S., Glaise, D., Zanninelli, G., Bilodeau, M., Loyer, P., Guguen-Guillouzo, C., and Baffet, G. (1999) The mitogen-activated protein kinase kinase/extracellular signal-regulated kinase cascade activation is a key signalling pathway involved in the regulation of G_1 phase progression in proliferating hepatocytes. *Mol. Cel. Biol* **19,** 6003–6011

25. Nelsen, C. J., Rickheim, D. G., Tucker, M. M., Hansen, L. K., and Albrecht, J. H. (2003) Evidence that cyclin D1 mediates both growth and proliferation downstream of TOR in hepatocytes. *J. Biol. Chem.* **278,** 3656–3663

26. Li, W., Liang, X., Kellendonk, C., Poli, V., and Taub, R. (2002) STAT3 contributes to the mitogenic response of hepatocytes during liver regeneration. *J. Biol. Chem.* **277,** 28411–28417

27. Yang, S. Q., Lin, H. Z., Mandal, A. K., Huang, J., and Diehl, A. M. (2001) Disrupted signaling and inhibited regeneration in obese mice with fatty livers: Implications for nonalcoholic fatty liver disease pathophysiology. *Hepatology* **34,** 694–706

28. Schwabe, R., Bradham, C. A., Uehara, T., Hatano, E., Bennett, B. L., Schoonhoven, R., and Brenner, D. A. (2003) c-Jun-N-Terminal kinase drives cyclin D1 expression and proliferation during liver regeneration. *Hepatology* **37,** 824–832

29. Coqueret, O. (2002) Linking cyclins to transcriptional control. *Gene* **299,** 35–55

30. Santamaría, E., Avila, M. A., Latasa, M. U., Rubio, A., Martín-Duce, A., Lu, S. C., Mato, J. M., and Corrales, F. J. (2003) Functional proteomics of non-alcoholic steatohepatitis: mitochondrial proteins as targets of S-adenosylmethionine. *Proc. Nat. Acad. Sci. USA.* **100,** 3065–3070

31. Majano, P. L., Garcîa-Monzûn, C., Garcîa-Trevijano, E. R., Corrales, F. J., Câmara, J., Ortiz, P., Mato, J. M., Avila, M. A., and Moreno-Otero, R. (2001) S-Adenosylmethionine modulates inducible nitric oxide synthase gene expression in rat liver and isolated hepatocytes. *J. Hepatol.* **35,** 692–699

32. Tombes, R. M., Auer, K. L., Mikkelsen, R., Valerie, K., Wymann, M. P., Marshall, C. J., McMahon, M., and Dent, P. (1998) The mitogen-activated protein (MAP) kinase cascade can either stimulate or inhibit DNA synthesis in primary cultures of rat hepatocytes depending upon whether its activation is acute/phasic or chronic. *Biochem. J.* **330,** 1451–1460

33. Factor, V. M., Jensen, M. R., and Thorgeirsson, S. S. (1997) Coexpression of c-myc and transforming growth factor alfa in the liver promotes early replicative senescence and diminishes regenerative capacity after partial hepatectomy in transgenic mice. *Hepatology* **26,** 1434–1443

Received October 31, 2003; accepted February 11, 2004.

Table 1

Hepatic SAMe levels during liver regeneration[a]

Time after 2/3 PH	SAMe level (nmol/mg protein)	
	WT	KO
24 h	0.95±0.07	0.70±0.09
36 h	0.62±0.05[b]	0.75±0.06
48 h	0.53±0.03[b]	0.61±0.06

[a]Results represent mean ± SE from three regenerating livers from wild-type (WT) and knockout (KO) animals for each time point. Hepatic SAMe levels were determined as described in Materials and Methods.
[b]$P < 0.05$ vs. WT at 24 h by ANOVA followed by Fisher's test.

Fig. 1

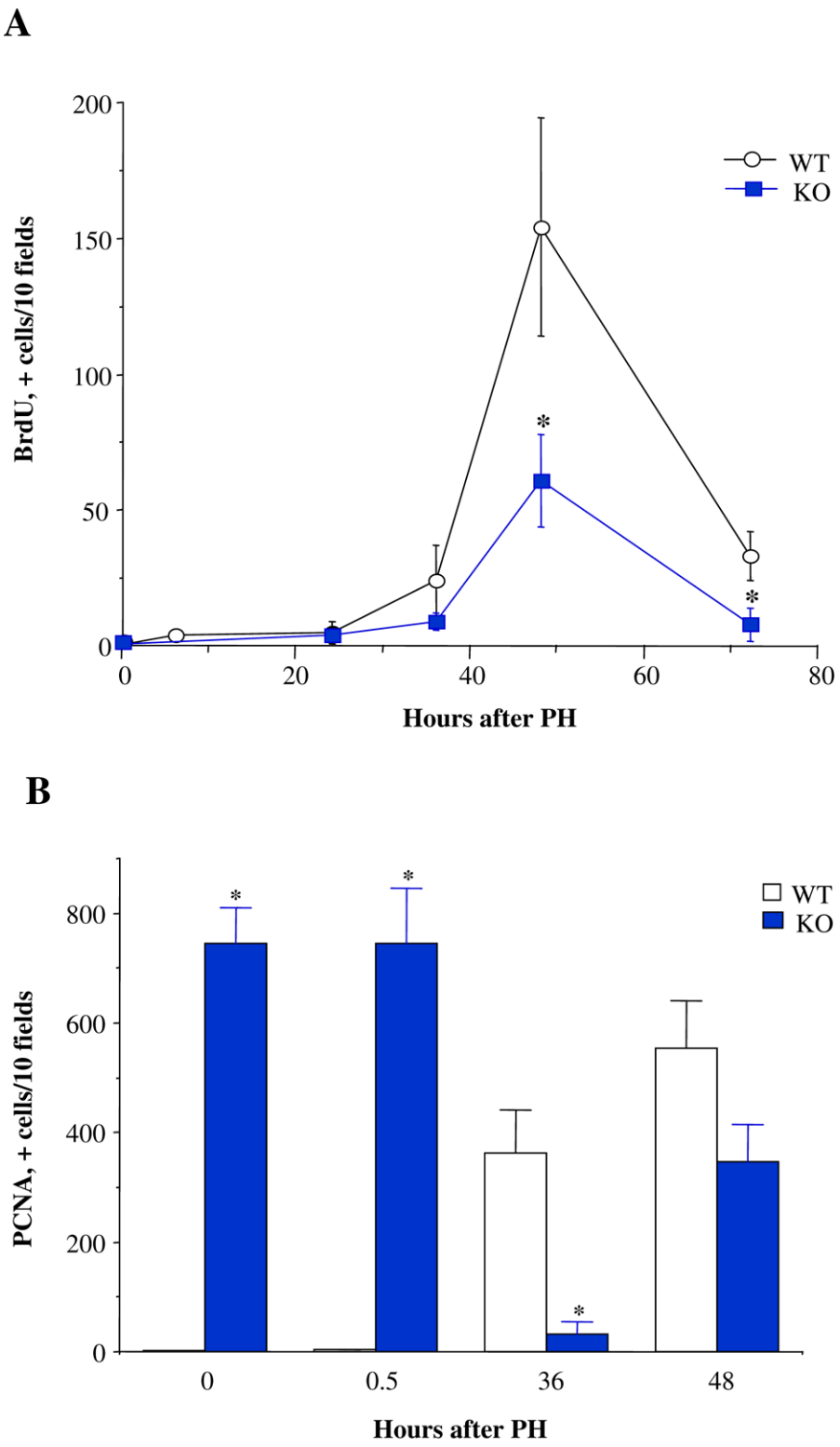

Figure 1. Hepatocyte replication after PH as assessed by BrDU incorporation (*A*) or PCNA staining (*B*). Mice were injected with BrDU intraperitoneally 2 h before sacrifice as described in Materials and Methods. BrDU and PCNA immunohistochemistry and morphometric analysis were done as described in Materials and Methods using formalin-fixed and paraffin-embedded liver tissues. Results are expressed as mean ± SE from three to six wild-type (WT) and knockout (KO) mice at each time point. *$P < 0.05$ vs. WT.

Fig. 2

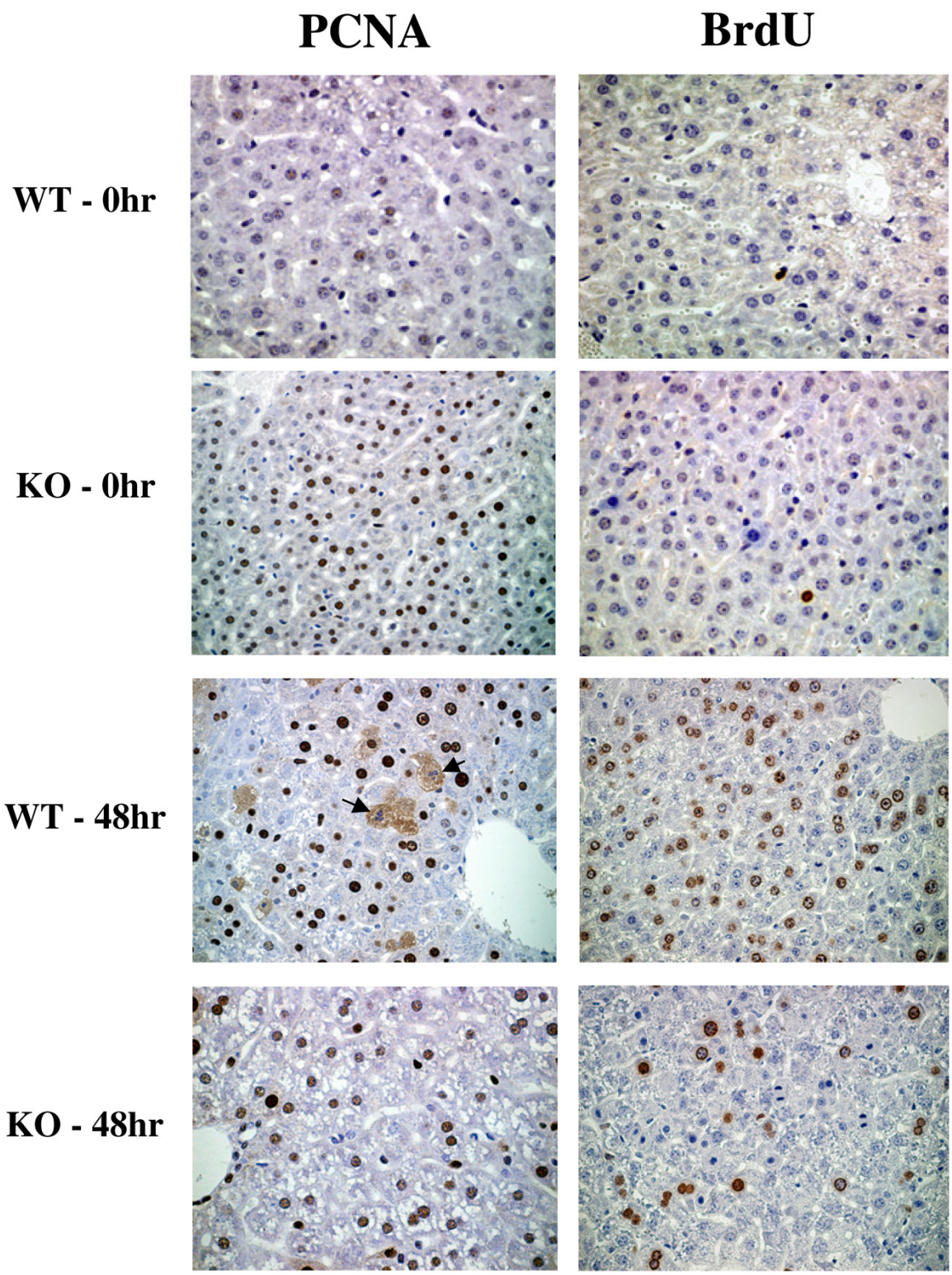

Figure 2. Representative immunohistology from wild-type (WT) and knockout (KO) mice. Note the intense PCNA staining at 0 h in the KO, which decreased at 48 h. In contrast, baseline PCNA expression is minimal in the WT, but many mitotic figures are seen at 48 h (arrows). BrDU incorporation (brown color stained nuclei) is nil at baseline in both types of mice and is much lower in the KO at 48 h. Hematoxylin and eosin ×400.

Fig. 3

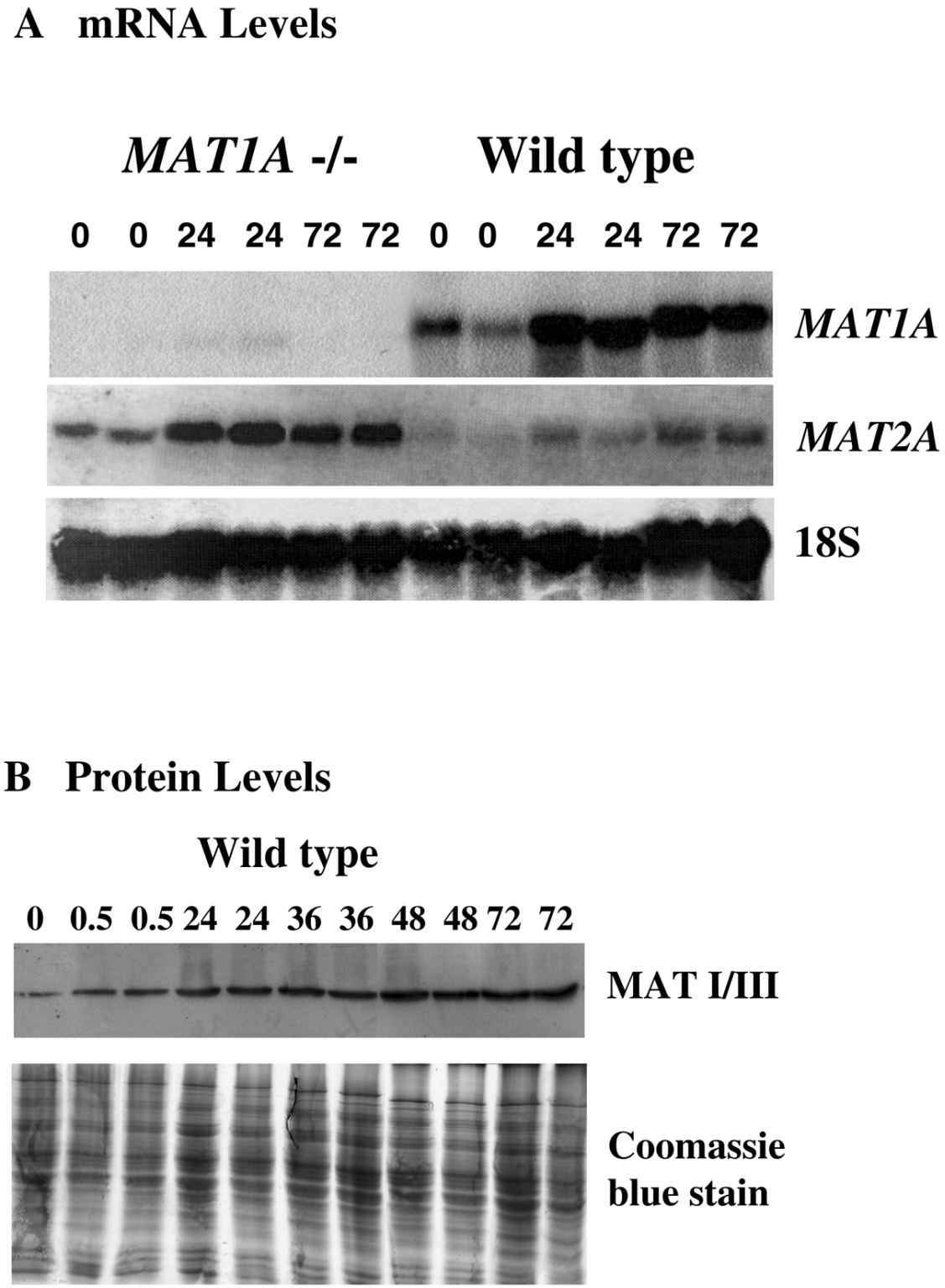

Figure 3. Northern (*A*) and Western blot (*B*) analysis of hepatic MAT during liver regeneration in the *MAT1A* knockout (–/–) and wild-type mice. Mice underwent 2/3 PH and were sacrificed at various times (0.5–72 h). Liver removed at the time of PH was used for baseline (0 time). Northern blot analysis was done using specific *MAT1A* and *MAT2A* cDNA probes as described in Materials and Methods. Membranes were sequentially probed with *MAT1A*, *MAT2A*, and 18S rRNA. Representative blots are shown. Western blot analysis was done using anti-MAT I/III antibodies using 50 µg liver homogenates from various time points (0–72 h). Representative blots are shown.

Fig. 4

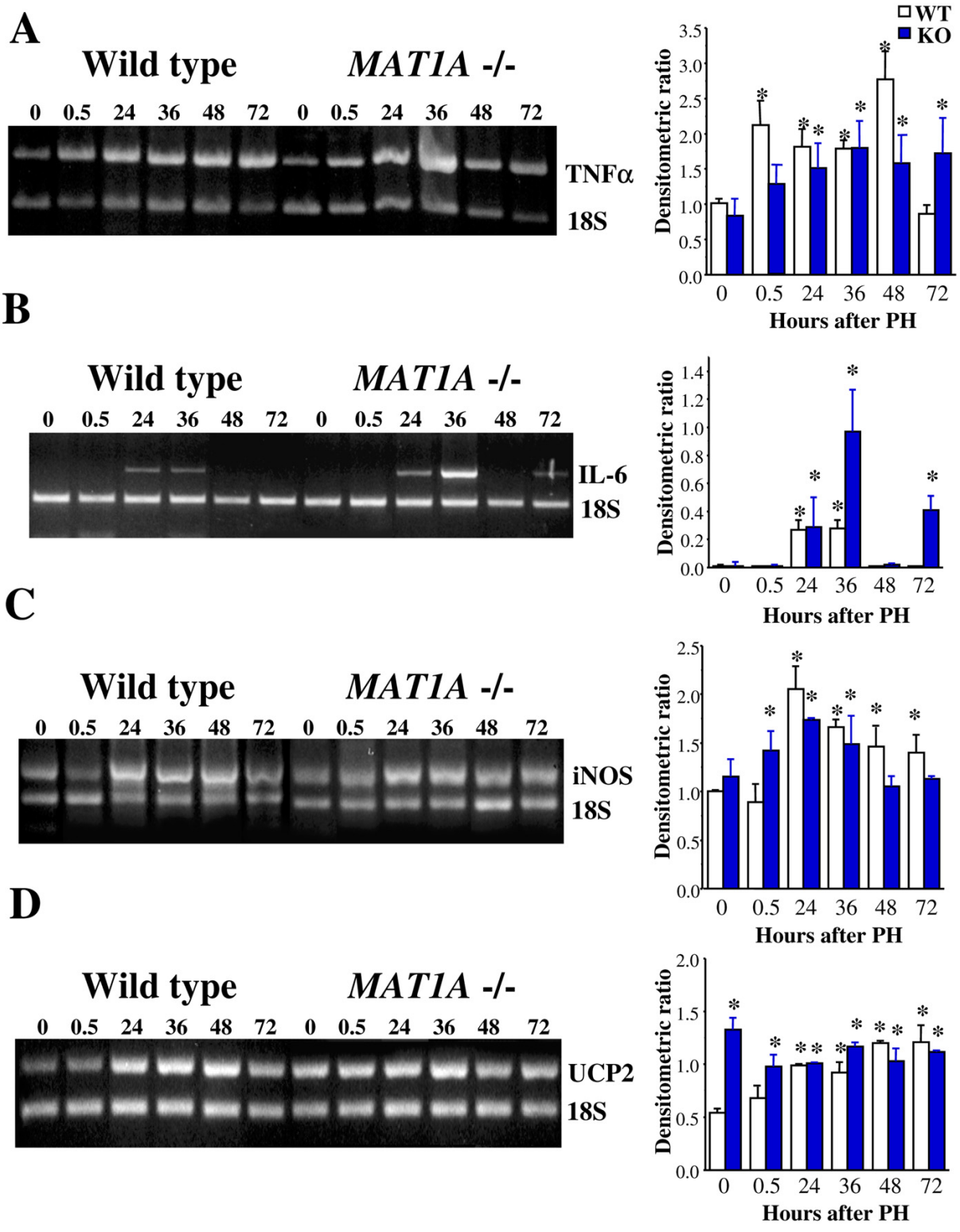

Figure 4. RT-PCR of TNF-α, IL-6, iNOS, and UCP2 in livers of *MAT1A* knockout (–/–) and wild-type mice. Mice were sacrificed at various times (0.5–72 h) following PH as described in Materials and Methods. Liver removed at the time of PH was used for baseline (0 time). Representative RT-PCRs are shown. Densitometric changes are shown in the right panels, expressed as the ratio of the gene of interest over 18S. *$P < 0.05$ vs. wild type at time 0.

Fig. 5

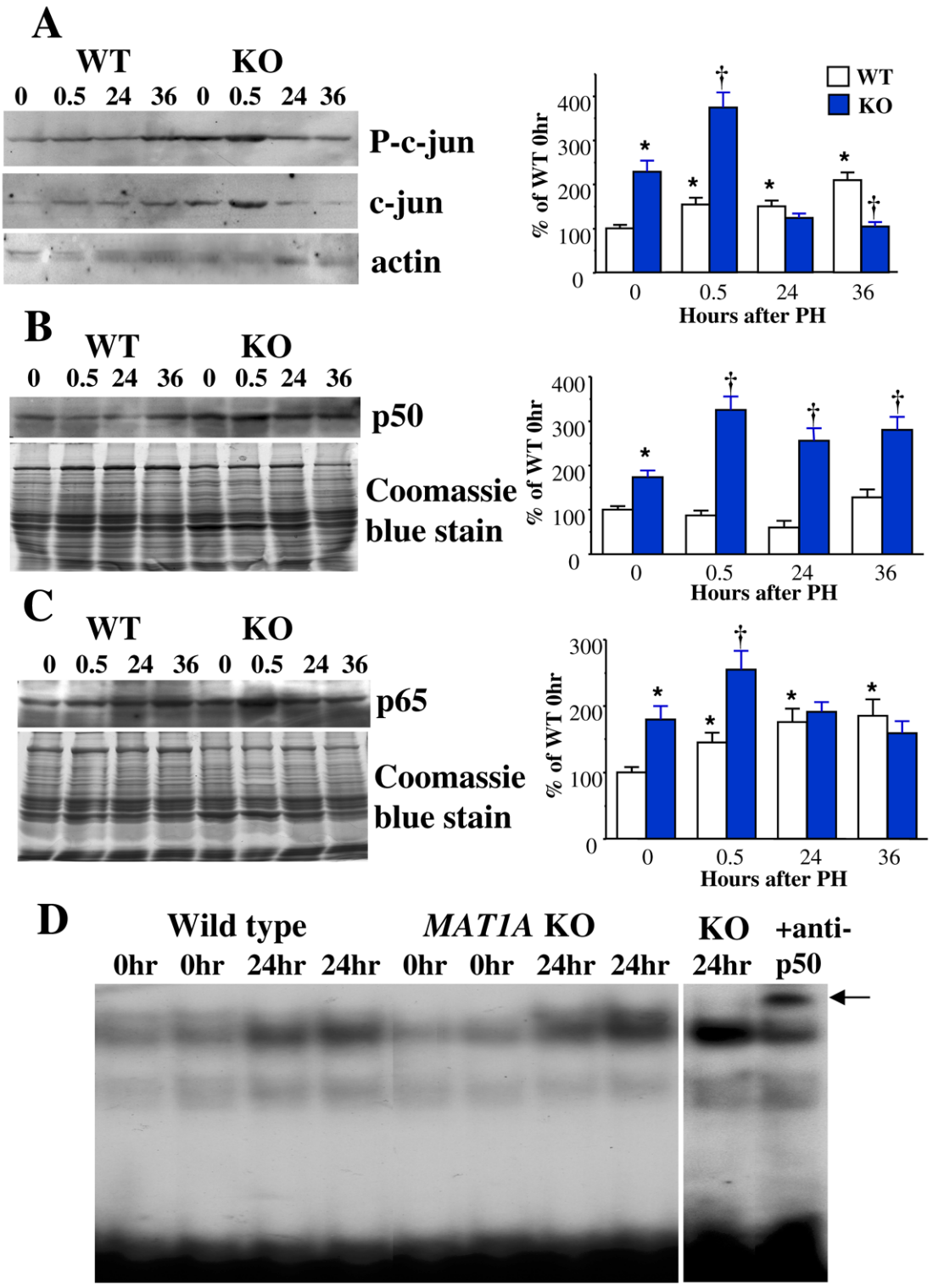

Figure 5. Western blot analysis of phospho-c-jun (P-c-jun), total c-jun (*A*), p50 (*B*), and p65 (*C*) in livers of *MAT1A* knockout (KO) and wild type (WT) mice. Mice were sacrificed at various times (0.5–36 h) following PH as described in Materials and Methods. Liver removed at the time of PH was used for baseline (0 time). Representative Western blots are shown. Densitometric changes are shown in the right panels, expressed as % of WT value at 0 h. EMSA with supershift analysis of NFκB nuclear binding activity in two WT and two KO mice at baseline and 24 h after PH was performed as described in Materials and Methods using 10 μg of nuclear protein each (***D***). *$P < 0.05$ vs. WT at time 0, $^{\dagger}P < 0.05$ vs. WT at respective time points.

Fig. 6

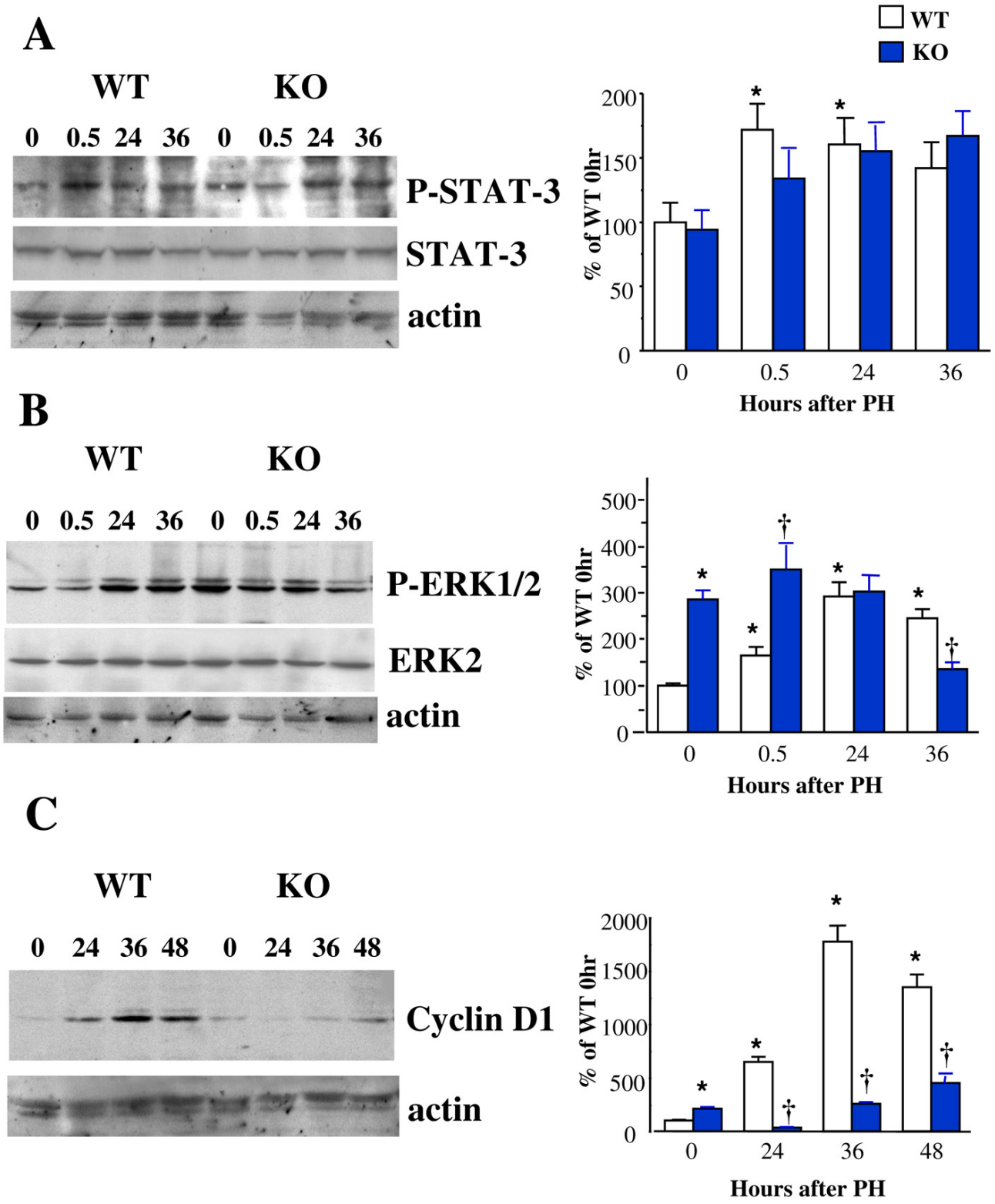

Figure 6. Western blot analysis of phospho-STAT-3 (P-STAT-3), total STAT-3, phospho-ERK1/2 (P-ERK1/2), total ERK2, and cyclin D1 in livers of *MAT1A* knockout (KO) and wild-type (WT) mice. Mice were sacrificed at various times (0.5–36 h for P-STAT-3 and P-ERK1/2, 0–48 h for cyclin D1) following PH as described in Materials and Methods. Liver removed at the time of PH was used for baseline (0 time). Representative Western blots are shown. Densitometric changes are shown in the right panels, expressed as % of WT value at 0 h. *$P < 0.05$ vs. WT at time 0, $^{\dagger}P <$ 0.05 vs. WT at respective time points.

Fig. 7

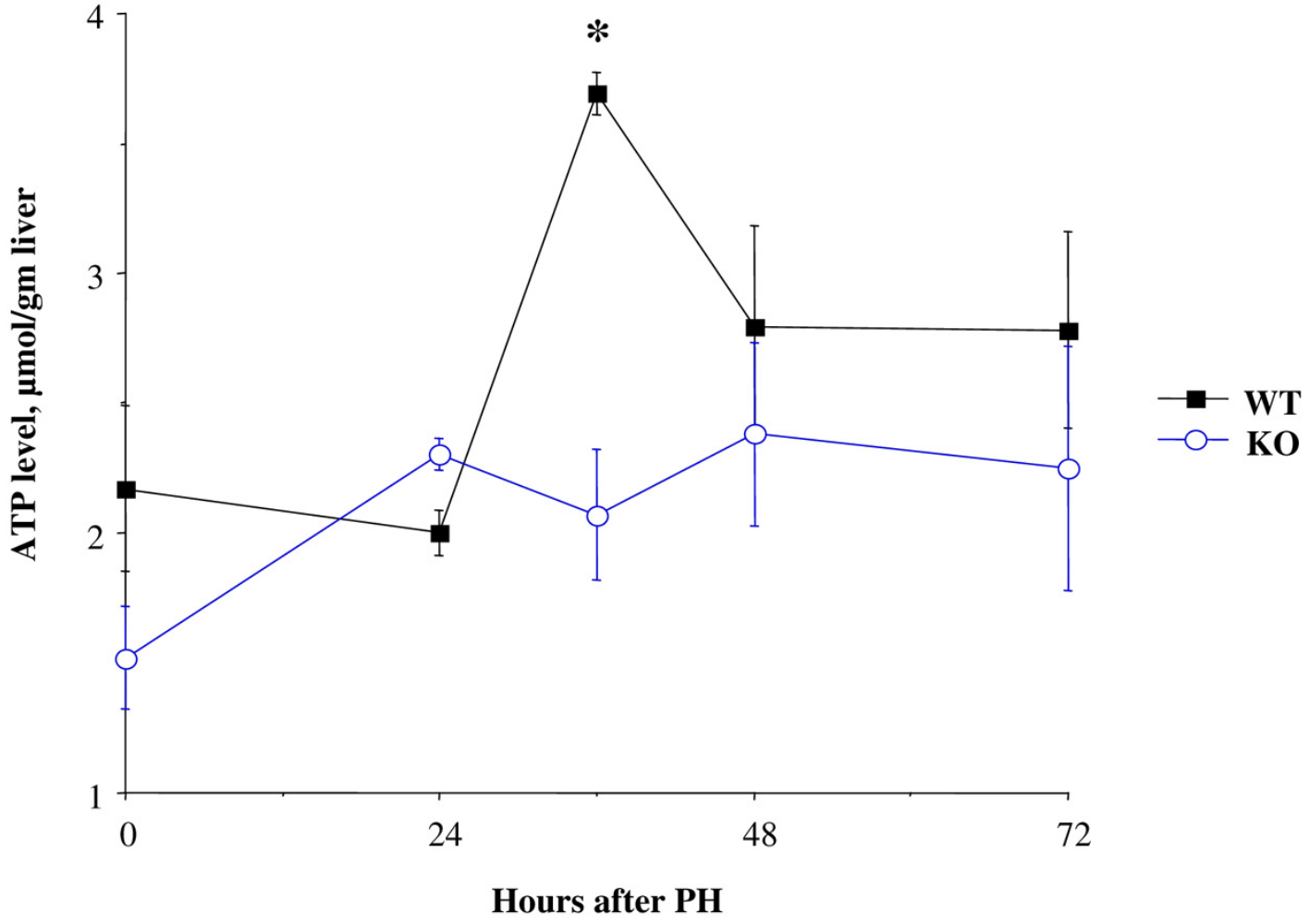

Figure 7. Changes in ATP content in livers of *MAT1A* knockout (KO) and wild-type (WT) mice. Mice were sacrificed at various times (24, 36, 48, and 72 h) following PH. Hepatic ATP levels were measured as described in Materials and Methods. Liver removed at the time of PH was used for baseline (0 time). Results are expressed as mean ± SE from three WT and three KO mice at each time point. *$P < 0.05$ vs. WT.

Fig. 8

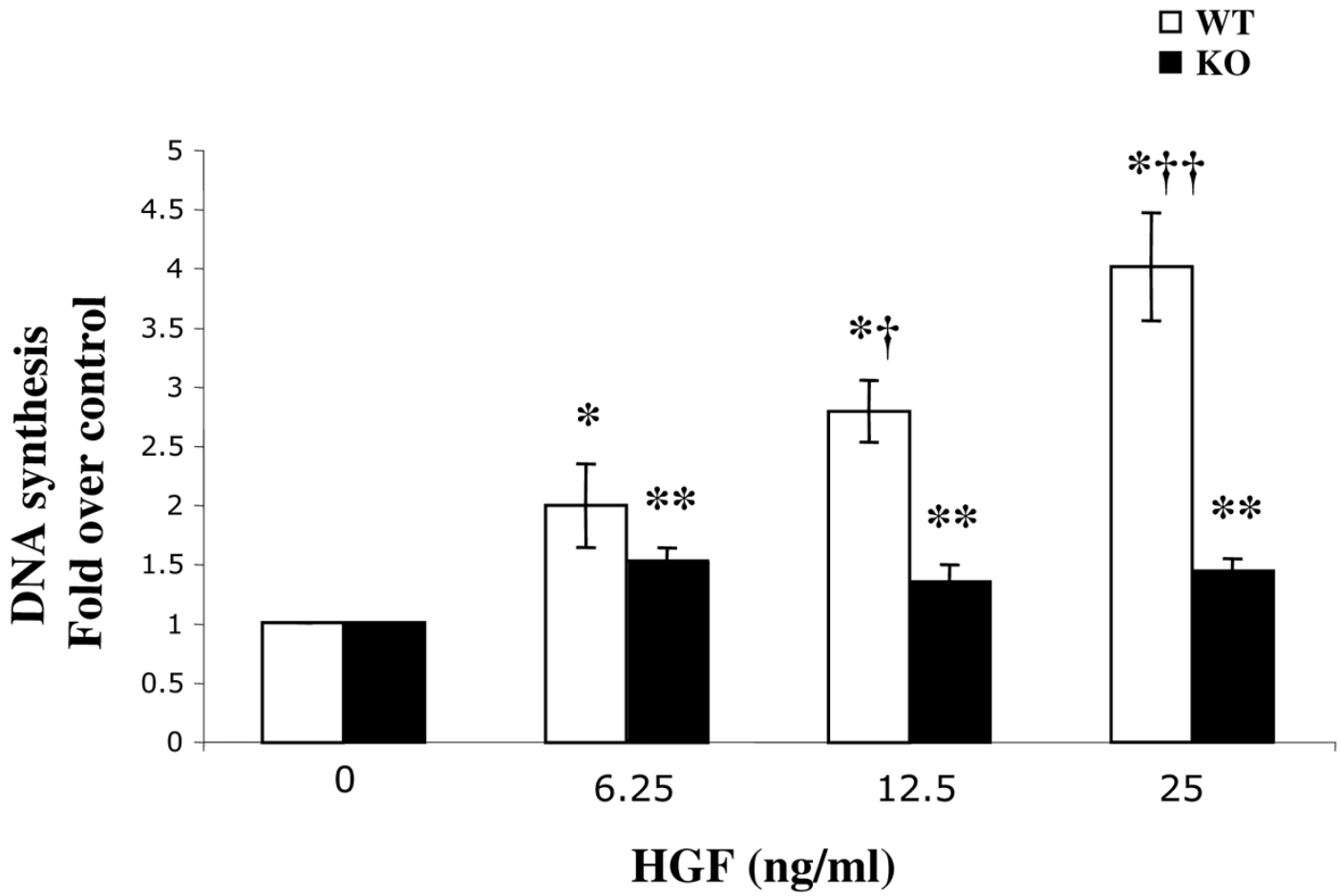

Figure 8. DNA synthesis in *MAT1A* knockout (KO) and wild-type (WT) hepatocytes in response to HGF. Hepatocytes were isolated from 3-month-old KO and WT animals and cultured as described in Materials and Methods. DNA synthesis was measured after treatment with varying concentrations of HGF. Results are expressed as mean ± SD from triplicates. Values found in either WT or KO control hepatocytes (HGF untreated cells) were arbitrarily given the value of one. *$P < 0.05$ vs. WT control hepatocytes, **$P < 0.05$ vs. KO control hepatocytes and WT hepatocytes at respective HGF doses, $^{\dagger}P < 0.05$ vs. WT treated with HGF 6.25 ng/ml, $^{\dagger\dagger}P < 0.05$ vs. WT treated with HGF 12.5 ng/ml.